Distribution of Eu^{3+} Dopant Ions in C_{3i} and C_2 Sites of the Nanocrystalline Sc_2O_3:Eu Phosphor

Giorgio Concas[a], Giorgio Spano[a], Marco Bettinelli[b], and Adolfo Speghini[b]

[a] Dipartimento di Fisica, Università di Cagliari and CNISM, S. P. Monserrato-Sestu km 0.700, I-09042 Monserrato (CA), Italy
[b] Dipartimento Scientifico e Tecnologico, Università di Verona and INSTM, UdR Verona, Ca′ Vignal, Strada le Grazie 15, I-37134 Verona, Italy

Reprint requests to Prof. G. C.: Fax: +39070510171; E-mail: giorgio.concas@dsf.unica.it

Z. Naturforsch. **63a,** 210 – 216 (2008); received September 21, 2007

The actual occupancy of the two available cation sites by luminescent Eu^{3+} ions, in the cubic bixbyite-type structure of nanocrystalline sesquioxides, has been investigated by ^{151}Eu Mössbauer spectroscopy and magnetic susceptibility measurements. It was found that one fourth of the europium ions is in the more symmetric site C_{3i} and three fourths in the less symmetric site C_2; the distribution is random. In the series of the Eu-doped sesquioxides Sc_2O_3, Lu_2O_3, Y_2O_3 and Eu_2O_3, the covalency of the Eu-O bond and the Eu site distortion increase with the difference in ionic radii between europium and the cation of the host compound. The magnetic susceptibility has been analyzed as sum of the contributions of the free Eu^{3+} ion, of the crystal-field effect and of the exchange interaction between europium ions.

Key words: Europium; Oxides; Nanocrystals; Mössbauer Spectroscopy; Structural Properties.

1. Introduction

Nanocrystalline oxide materials activated with trivalent lanthanoide ions (Ln^{3+}) are becoming increasingly important due to their valuable luminescence properties, which make them interesting for several advanced applications, such as innovative phosphors [1] and materials for optical imaging in biomedicine [2]. In this broad class of materials, particular attention has been devoted to the study of nanocrystalline cubic sesquioxides, which combine a relatively easy preparation with several favourable physical properties [3, 4]. Among the activator ions, particular attention has been payed to Eu^{3+}, which gives rise to efficient red luminescence, and can be used as a useful spectroscopic probe of the environment surrounding the Ln^{3+} ions [5].

In the case of cubic sesquioxides with the structure of Y_2O_3, the constituting cations are located in two non-equivalent special positions: 24d (site symmetry C_2) and 8b (site symmetry C_{3i}) [6]. In principle, the luminescent ion Eu^{3+} may replace the cations in a random or preferential way. The distribution of Eu^{3+} in bulk compounds has been subject of theoretical and experimental work. Recently Stanek et al. [7] performed atomic scale simulations and foresaw a preferential occupation of the C_{3i} site when the Eu^{3+} ion is larger than the host lattice cation. The results of the simulations were compared with the experimental investigations of bulk samples of doped Y_2O_3 and Lu_2O_3 by means of X-ray diffraction [8] and ^{151}Eu Mössbauer spectroscopy [9, 10]; by the experiments a random distribution of Eu in bulk Y_2O_3 [8, 9] and a preferential occupation of the C_2 site in bulk Lu_2O_3 was found [10]. The magnetic susceptibility measurements also gave information about the Eu distribution [8, 11]; the published results will be discussed in Section 4.

In the isostructural series Sc_2O_3, Y_2O_3, Lu_2O_3, in which the cations have a closed shell, Sc^{3+} has the smallest ionic radius; it is interesting to investigate the distribution of the luminescent Eu^{3+} dopant ion in nanocrystalline cubic Sc_2O_3, whose structure, morphology and luminescence has recently been reported [12]. The nanocrystalline character of this compound does not permit the use of single crystal X-ray diffraction, which is the standard method of this kind of investigation.

^{151}Eu Mössbauer spectroscopy represents a valuable technique to investigate the features of the europium ion sites in crystalline and amorphous mate-

rials [13 – 15]. In some cases it can determine the relative amount of Eu in different crystallographic sites, because the probability of resonant absorption by a single ^{151}Eu nucleus is approximately equal for trivalent ions in different sites of the same compound; therefore the relative occupancy may be evaluated from the relative area of the components in the spectrum. In particular this is useful when the two sites have different symmetry, because this spectroscopy gives direct information about the site symmetry.

In fact, the gamma ray from ^{151}Eu is emitted during a transition from an excited state with spin 7/2 to the ground state with spin 5/2 [13]. If there is no threefold or fourfold symmetry axis passing through the nucleus, the components of the electric field tensor along the principal axes are different, the asymmetry parameter η is non-zero [16], and there are 12 allowed transitions. If a threefold or fourfold axis is present, the asymmetry parameter is zero and 8 transitions are observed. In a compound with two mutually perpendicular axes of threefold or higher symmetry, the electric field gradient [and therefore the quadrupole interaction (QI) parameter] is zero and a single transition is observed [13].

The discrimination of the contribution of different sites occupied by Eu^{3+} is limited by experimental factors: the difference of isomer shift (IS) is usually smaller than the line width and comparable with the quadrupolar splitting. Therefore in the spectrum only a single absorption peak appears; it may be resolved into two contributions of the sites, each splits by the quadrupolar interaction, using a suitable fitting procedure.

Bulk cubic sesquioxides doped with Eu have also been investigated by Mössbauer spectroscopy by Hintzen and van Noort [17]. A resolution of the contribution of the two different sites is proposed, which uses a fitting of the spectra with two single Lorentzian curves, i. e. without quadrupole splitting; the ratio of the areas of the two contributions is usually fixed [17].

The aim of this study is to evaluate the actual occupancy of the two available cation sites in the cubic structure of nanocrystalline Sc_2O_3 by Eu^{3+} ions. To this end we resolve in the absorption spectrum the contribution of different crystalline sites that may be occupied by trivalent europium, allowing for the quadrupole interaction. The hyperfine parameters will be discussed in terms of symmetry and bonding of the lanthanoide ion; moreover, the evolution of the parameters vs. ionic radii in a series of sesquioxides with the same bixbyite-type structure will be presented. The Mössbauer spectroscopic study is justified by the consideration that the X-ray powder diffraction investigation, reported in [12], did not solve the question about the site occupancy by Eu^{3+}. The magnetic susceptibility values, measured at 2 K and 290 K, will be discussed in connection with the Eu distribution and the crystal field (CF) of the Eu sites in the different host lattices.

2. Experimental

The nanocrystalline $Sc_{1.8}Eu_{0.2}O_3$, $Lu_{1.8}Eu_{0.2}O_3$ and $Y_{1.8}Eu_{0.2}O_3$ samples were prepared by propellant synthesis as described in [12, 18, 19]. Bulk cubic Eu_2O_3 was prepared by heating commercial Eu_2O_3 (Aldrich, 99.99%) at 1000 °C for 6 h [20].

Mössbauer absorption spectra were obtained in standard transmission geometry, using a source of $^{151}SmF_3$ with the activity 3.7 GBq. A calibration was performed using a source of ^{57}Co in rhodium and a metallic iron foil (25 μm thick) as the absorber. The isomer shift of the samples was measured using anhydrous EuF_3 as reference material. The measurements were carried out at room temperature on a powder sample with an absorber thickness of 3.8 mg/cm^2 of Eu; this value corresponds to an effective thickness of $t = 1$, when calculated using the recoilless fraction of the source, $f = 0.6$ [13]. The powders were contained in a Plexiglas holder. The Eu_2O_3 powder was mixed with graphite in order to spread it uniformly over the bottom of the sample holder. In order to obtain the same quality of the spectra, the acquisition has been carried out to obtain a relative experimental error of about 0.005% on the maximum resonant absorption.

The first step of the analysis of complex spectra was the determination of the full width at half maximum (FWHM) of the crystalline absorption peak for spectra obtained with our $^{151}SmF_3$ source. The elpasolite $Cs_2NaEuCl_6$ crystal contains Eu^{3+} in an octahedral site (cubic symmetry) [21]. It permits to verify that the emission line of our source could be treated as monochromatic (unsplit), because Eu^{3+} in a site of cubic symmetry gives a single absorption line if the source is monochromatic [13]. The elpasolite crystal was also used in order to measure the line width of our source using the trivalent europium in a crystalline environment. The FWHM of the absorption peak has been measured with an effective absorber thickness of $t = 1$; the obtained value was (1.76 ± 0.01) mm/s

with $t = 1$. The line width was also measured using absorbers of $Cs_2NaEuCl_6$ with the effective thickness $t = 0.5$ and $t = 2$. The resulting FWHM as a function of the thickness t follows the linear behaviour $\Gamma = \Gamma_0 + at$ predicted by the theory [16, 22]; the linear fit of the experimental data gave an FWHM at zero thickness of $\Gamma_0 = (1.705 \pm 0.003)$ mm/s and a variation coefficient of $a = (0.052 \pm 0.003)$ mm/s.

The absorption spectra were analyzed by fitting the data with curves of Lorentzian shape, allowing for the quadrupole interaction when present. We used the method for the analysis of pure quadrupole spectra proposed by Shenoy and Dunlap [23], with a value of the quadrupole ratio of $R = 1.312$ [24]. The thickness of the absorbers permitted the use of a Lorentzian line shape, because the thin absorber approximation could be used (thickness less than 6 mg/cm^2 of Eu) [22, 25]. When the QI is present, we used a quadrupole multiplet of Lorentzian curves; it is made up of 12 components if $\eta \neq 0$, and 8 components if $\eta = 0$. The FWHM of the Lorentzian curves in the fit of the spectra has been fixed to the value $\Gamma = 1.76$ mm/s measured with the elpasolite crystal for an effective thickness of $t = 1$.

The quality of the fits was tested using the usual chi-squared test and a weighted form of the Durbin-Watson d statistics, that was used in the Rietveld analysis of powder diffraction data and in the analysis of Mössbauer spectra [26, 14]. The parameter d quantifies the serial correlation between adjacent least-squares residuals, while Q_d depends on the number of data and of least-squares parameters; if $|d-2| < |Q_d-2|$, consecutive residuals are insignificantly correlated and the experimental data are randomly distributed around the fit curve.

The magnetic susceptibility measurements were performed using a Quantum Design MPMS5 XL5 SQUID magnetometer calibrated with a Pd standard; the linearity of the magnetization vs. applied field was verified by measuring the magnetization at 2 K and 290 K with fields from 0.02 to 50 kOe. The measurements were carried out on powder samples of 50 mg, embedded in a Teflon tape.

3. Results

Detailed analyses of the powder X-ray diffraction (XRD) patterns have been published by some of the authors for the nanocrystalline europium-doped scandia [12], lutetia [18] and yttria [19]. The XRD of nanocrystalline $Sc_{1.8}Eu_{0.2}O_3$ confirms that the sample is single-phase with the cubic structure with the cell parameter $a = 0.99170(1)$ nm, slightly larger than for the undoped nanocrystalline Sc_2O_3 [12]; the average crystallite size, determined from the profile analysis of the XRD line using the Warren-Averbach method, is 14 nm with no significant microstrain [12]. Eu-doped and undoped Sc_2O_3 nanopowders have been fully characterized by transmission electron microscopy images, showing that the average crystallite size is 22 and 40 nm, respectively [12]. XRD results show that Eu^{3+}-doped Y_2O_3 and Lu_2O_3 nanopowders are single-phase with a cubic structure [$a = 1.0649(2)$ nm and $a = 1.03901(4)$ nm, respectively], and that the average crystallite size is 10 nm and 34 nm, respectively [18, 19]. The bulk Eu_2O_3 sample shows the cubic structure [$a = 1.086(1)$ nm] [6], as confirmed by powder XRD.

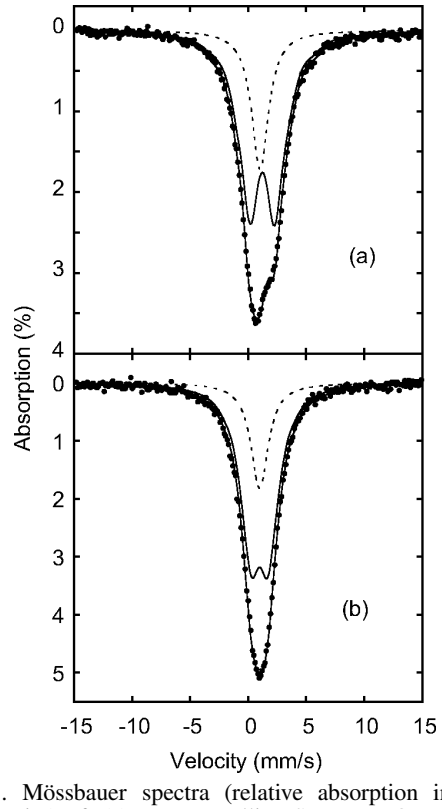

Fig. 1. Mössbauer spectra (relative absorption intensity vs. velocity) of: (a) nanocrystalline $Sc_{1.8}Eu_{0.2}O_3$; (b) bulk Eu_2O_3. The experimental data (dots) and the fit curve (full line) are shown along with the components associated to the C_{3i} and C_2 sites (dashed line and full line, respectively).

The Mössbauer spectrum of nanocrystalline cubic $Sc_{1.8}Eu_{0.2}O_3$ is shown in Figure 1a. This compound needs a suitable fitting procedure which discriminates,

Sample	δ, mm/s	eQV_{zz}, mm/s	η	*Area*, %	*d*	Q_d	χ^2
nano-$Sc_{1.8}Eu_{0.2}O_3$					1.47	1.65	1.27
C_{3i}	1.18(1)	0		26(1)			
C_2	1.38(1)	−12.6(1)	1.0(1)	74(1)			
bulk Eu_2O_3					1.67	1.65	1.26
C_{3i}	1.03(1)	0		24(1)			
C_2	1.03(1)	−8.6(1)	1.0(1)	76(1)			
nano-$Lu_{1.8}Eu_{0.2}O_3$					1.78	1.65	1.02
C_{3i}	1.23(1)	0		25(1)			
C_2	1.23(1)	−10.4(2)	1.0	75(1)			
nano-$Y_{1.8}Eu_{0.2}O_3$					1.79	1.65	1.18
C_{3i}	1.14(1)	0		27(3)			
C_2	1.14(1)	−9.4(4)	1.0	73(3)			

Table 1. Mössbauer parameters obtained by fitting the spectra. δ is the isomer shift with respect to EuF_3, eQV_{zz} is the quadrupole interaction parameter, η is the asymmetry parameter and *Area* is the relative area of the components. The *d*, Q_d Durbin-Watson and χ^2 parameter are also reported. The FWHM of the Lorentzian curves has been fixed to 1.76 mm/s. Statistical errors are given in parenthesis as errors on the last digit.

in the spectrum, the contribution of the C_{3i} and C_2 sites; a good procedure will give, as result of the fitting, two components with a ratio of the areas corresponding to the actual occupancy of the sites. The simple use of two quadrupole multiplets with free parameters is not possible because the large number of parameters makes the fitting unstable.

A suitable fitting procedure has been tested using a cubic Eu_2O_3 sample [9], because this compound has the same bixbyite-type structure of Sc_2O_3 and other sesquioxides (Y_2O_3 and Lu_2O_3) and a known occupancy of the C_{3i} and C_2 sites by europium. The experimental spectrum of Eu_2O_3 was well fitted using two contributions corresponding to the two sites; in this procedure the asymmetry parameter of the C_{3i} site has been fixed to zero, because of the threefold axis of symmetry, and the FWHM of the multiplets has been fixed to the crystalline width ($\Gamma = 1.76$ mm/s for $t = 1$). In order to reduce the number of free parameters, the value of IS of the sites has been forced to take the same variable value, and the QI parameter of the more symmetric site has been fixed to zero, because some trial fits showed that the value of IS of the two sites is about the same and the QI of the C_{3i} site is very small; these constraints do not worsen the fit. The equality of the IS is reasonable because the average Eu-O distance of the two sites is equal, while the smallness of the QI in the C_{3i} site is caused by the equal value of the six Eu-O distances [27]. The resulting calculated curve is shown in Fig. 1b with the components separately; the fit parameters are given in Table 1. The relative areas of the components (24% for C_{3i} and 76% for C_2) give the right number of occupied sites (25% and 75%) within the experimental error. This fitting procedure has been applied to the spectra of the nanocrystalline cubic lutetia and yttria samples which are shown in Fig. 2a and

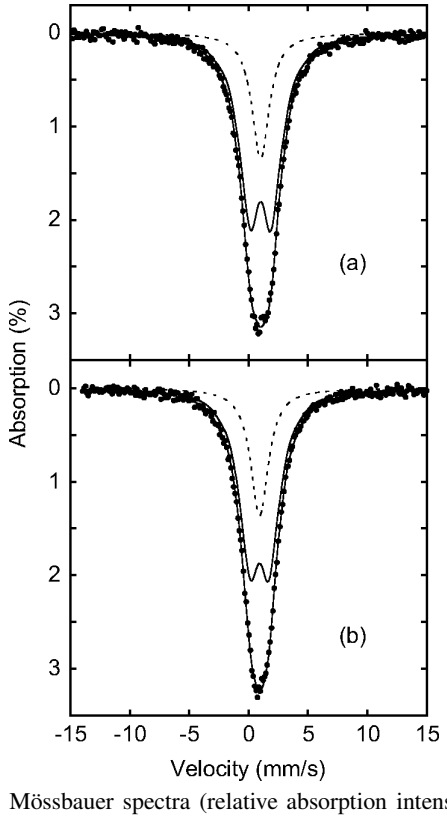

Fig. 2. Mössbauer spectra (relative absorption intensity vs. velocity) of: (a) nanocrystalline $Lu_{1.8}Eu_{0.2}O_3$; (b) nanocrystalline $Y_{1.8}Eu_{0.2}O_3$. The experimental data (dots) and the fit curve (full line) are shown along with the components associated to the C_{3i} and C_2 sites (dashed line and full line, respectively).

Fig. 2b with the fit curves; the parameters obtained by the fitting procedure are reported in Table 1 [9]. It results that in both cases, the europium ion occupies the C_{3i} and the C_2 sites with a probability equal to the relative number of sites within the experimental error [9].

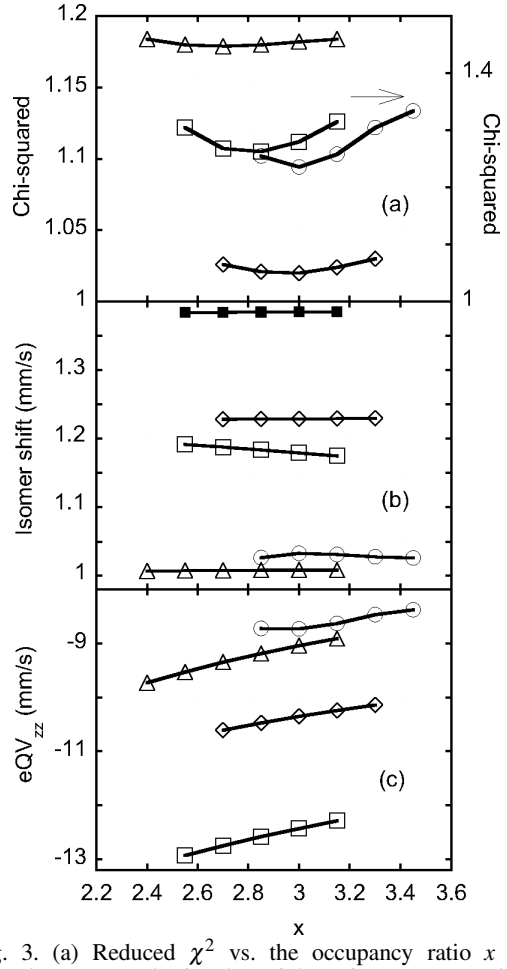

Fig. 3. (a) Reduced χ^2 vs. the occupancy ratio x (left axis: lozenges and triangles; right axis: squares and circles); (b) isomer shift vs. x; (c) QI parameter vs. x. The evolution of the parameters for $Sc_{1.8}Eu_{0.2}O_3$ (open squares and closed squares for the 2nd IS), Eu_2O_3 (open circles), $Lu_{1.8}Eu_{0.2}O_3$ (open lozenges) and $Y_{1.8}Eu_{0.2}O_3$ (open triangles) are shown.

Differently from the spectra of Eu_2O_3 (Fig. 1b) and other sesquioxides such as $Y_{1.8}Eu_{0.2}O_3$ and $Lu_{1.8}Eu_{0.2}O_3$ [9], the spectrum of $Sc_{1.8}Eu_{0.2}O_3$ is not symmetric; a trial fit of the data of $Sc_{1.8}Eu_{0.2}O_3$ with the same constraints used for the other samples gives a too large value of the chi-squared parameter ($\chi^2 = 3.5$) and a symmetric calculated curve. In order to take into account the asymmetry of the spectrum, we relaxed the constraint concerning the IS and made independent the IS of the two sites. The resulting calculated curve is shown in Fig. 1a with the components separately; the fit parameters are given in Table 1. The occupational probability of the C_{3i} and C_2 sites are 26% and 74%,

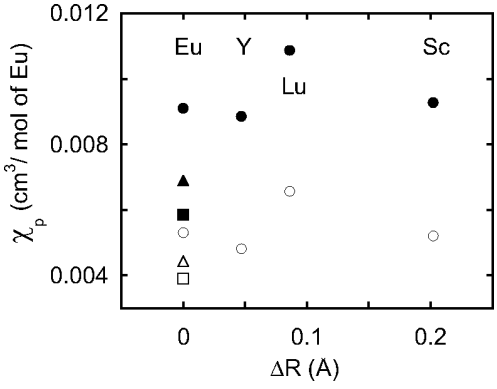

Fig. 4. Evolution of the paramagnetic susceptibility per mole of Eu (CGS system) vs. the difference of ionic radii $\Delta R = R_{Eu} - R_X$, where R_X is the ionic radius of the hexacoordinated trivalent ion (X = Eu, Y, Lu, Sc). The experimental susceptibilities of Eu_2O_3 and $X_{1.8}Eu_{0.2}O_3$ at 2 K (closed circles) and 290 K (open circles) are shown. The values, calculated by Huang and Van Vleck for Eu_2O_3 [29], of χ_{FI} (closed square at 2 K and open square at 290 K) and $\chi_{FI} + \chi_{CFE}$ (closed triangle at 2 K and open triangle at 290 K) are shown. The relative experimental error is 1%.

respectively, which agrees with the relative number of available sites within the experimental error.

In order to test the quality of the fits, the evolution of the reduced chi-squared vs. x has been investigated, with x defined as the occupancy ratio of the C_2 and C_{3i} sites. Several fits have been performed by fixing x to different values around $x = 3$ (random distribution). Considering that the value of x resulting from the fits reported in Table 1 is $x = 2.85 \pm 0.15$ for scandia, 3.17 ± 0.17 for europium oxide, 3.00 ± 0.16 for lutetia and 2.70 ± 0.41 for yttria, it is observable in Fig. 3a that the minima of chi-squared correspond to the values of x in Table 1, within the statistical uncertainty. Figures 3b and 3c show the corresponding evolution of the IS and of the QI parameter vs. x, respectively; the asymmetry parameter η gives a constant unitary value and therefore is not shown.

The main difference between $Sc_{1.8}Eu_{0.2}O_3$ and the sesquioxides of Eu, Y and Lu is the different value of IS of the two sites, which appears in the spectrum as lack of symmetry. From a structural point of view, the main difference is the small ionic size of scandium compared to europium; in fact, the trivalent ionic radius (IR) of Sc is 0.745 Å for the coordination number CN = 6, while it is 0.900 Å for Y and 0.861 Å for Lu, to be compared with 0.947 Å of Eu [28]. In the following the results are reported vs. the difference of ionic radii between Eu^{3+} and the cation of the host compound.

Figure 4 shows the paramagnetic susceptibility (PS) of the samples vs. the difference of ionic radii; the susceptibility per mole of Eu in the CGS system, at temperatures of 2 K and 290 K, is given. The PS has been calculated by subtracting the diamagnetic contribution of the ions [30].

4. Discussion

The PS χ_p in these oxides is due to the europium atom [8, 11, 31] and has been investigated by Huang and van Vleck in bulk Eu_2O_3 [29]:

$$\chi_p = \chi_{FI} + \chi_{CFE} + \chi_{ex}, \quad (1)$$

where χ_{FI} is the paramagnetic susceptibility of the free Eu^{3+} ion, χ_{CFE} is the contribution of the CF effect and χ_{ex} is due to the exchange coupling between the Eu^{3+} ions. The susceptibility has been used in the literature in order to determine the distribution of Eu in the two sites, starting from the consideration that χ_{CFE} associated with the more symmetric C_{3i} site is smaller than with the C_2 site [8, 11]; moreover χ_{ex} should be negligible for oxides doped with 10% of Eu [8, 11]. Therefore it is expected that the susceptibility of a doped oxide is about equal to $\chi_{FI} + \chi_{CFE}$ of Eu_2O_3 if the distribution is random and larger or smaller if there is a preferential occupancy of the C_2 or C_{3i} site, respectively [8, 11]. The values of χ_{FI} and $\chi_{FI} + \chi_{CFE}$ for Eu_2O_3 at 2 K and 290 K, calculated in [29], are shown in Figure 4. The calculated values for Eu_2O_3 will be denoted as χ_{FI,Eu_2O_3} and χ_{CFE,Eu_2O_3}, while χ_{p,Eu_2O_3} denotes the measured PS of Eu_2O_3. Antic et al. [8] measured $\chi_p = 4.5 \cdot 10^{-3}$ cm^3/mol for Eu in bulk $Y_{1.8}Eu_{0.2}O_3$ at room temperature; they concluded that it is consistent with a random distribution. Grill and Schieber [11] measured $\chi_p = 14.0 \cdot 10^{-3}$ cm^3/mol for Eu in bulk $Lu_{1.8}Eu_{0.2}O_3$ at 95 K; they explained the observed values with a preferential occupation of the C_2 site or with an increase of the CF strongly dependent on the unit cell dimensions.

The PS of the various oxides shown in Fig. 4 has a different behaviour compared to Eu_2O_3. The PS of $Y_{1.8}$ $Eu_{0.2}O_3$ is smaller than χ_{p,Eu_2O_3} but larger than $\chi_{FI,Eu_2O_3} + \chi_{CFE,Eu_2O_3}$, while the PS of $Lu_{1.8}Eu_{0.2}O_3$ is larger than χ_{p,Eu_2O_3}. The value of the doped lutetia may be explained only by an increase of the CF due to the decrease of the lattice constant; the term χ_{CFE} cannot increase to give a PS larger than that of Eu_2O_3 if there is only a redistribution of the Eu^{3+} ions. The value of the doped yttria is not inconsistent with a random distribution because the increase over the $\chi_{FI,Eu_2O_3} + \chi_{CFE,Eu_2O_3}$ value can be explained by the increase of the CF; this increase is smaller than in the doped lutetia which is in agreement with the evolution of the lattice constant. The susceptibility of $Sc_{1.8}Eu_{0.2}O_3$ is about equal to χ_{p,Eu_2O_3}; this result needs the investigation of the temperature dependence of the susceptibility to be explained.

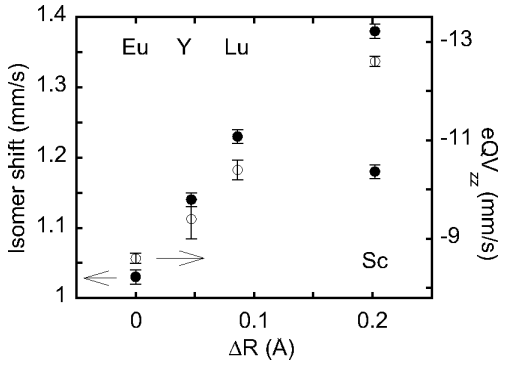

Fig. 5. Left axis (closed circles): evolution of the isomer shift vs. the difference of ionic radii $\Delta R = R_{Eu} - R_X$ (X = Eu, Y, Lu, Sc). Right axis (open circles): evolution of the quadrupole interaction parameter eQV_{zz} vs. the difference of ionic radii. Error bars are shown.

Figure 5 shows the evolution of the isomer shift vs. the difference of the ionic radii. The IS increases with the difference of the radii. The IS of trivalent europium varies from 0 mm/s, corresponding to the most ionic compound EuF_3, toward values larger than 1 mm/s as the covalency of the Eu-X bond increases [13]; therefore in our series the covalency of the Eu-O bond increases on decreasing the ionic radius of the host compound. It happens that the Eu^{3+} ion is squeezed in the Sc_2O_3 host; the shortest Eu-O distance corresponds to the highest covalency of the bond.

Moreover Fig. 5 shows the evolution of the QI parameter vs. the difference of IR; the absolute value of the QI parameter increases with the difference of the radii. Considering that the QI measures the distortion of the Eu site, this evolution points out that the large Eu ion causes the biggest site distortion in Sc_2O_3, which is the host compound with the smallest ion. The QI parameter is usually negative in trivalent europium oxides and varies from -5 mm/s to -13 mm/s [13]; the value of -12.6 mm/s of the Sc oxide points towards a strong distortion. The contribution to the distortion due to the difference of IR between Eu and Sc may be evaluated by comparing the value of -12.6 mm/s with -8.6 mm/s of Eu_2O_3.

On the basis of the analysis of the Mössbauer spectrum, the europium dopant ion in nanocrystalline cubic Sc_2O_3 is distributed between the C_{3i} and the C_2 site in a random way, without preferential occupancy. This is in qualitative agreement with the results of luminescence spectra recorded on the same sample in order to measure the asymmetry ratio of the integrated intensities of the $^5D_0 \rightarrow {}^7F_2$ and $^5D_0 \rightarrow {}^7F_1$ transitions, which is indicative of the asymmetry of the coordination polyhedron of the Eu^{3+} ion [12]: the lower the ratio value, the higher is the site symmetry of the Eu^{3+} ion. The obtained high asymmetry ratio value 5.3 ± 0.1 indicates that the local environment of the Eu^{3+} ion is notably distorted, which is in agreement with a C_2 symmetry for the sites mainly occupied by the dopant ions [12].

5. Conclusions

The relative area of the two contributions due to the Eu^{3+} ion in the C_{3i} and C_2 sites, in the spectrum of nanocrystalline $Sc_{1.8}Eu_{0.2}O_3$, shows that one fourth of the lanthanoide ions is in the more symmetric site and three fourths are in the less symmetric one; the distribution is random, without preferential occupancy. In a series of nanocrystalline sesquioxides with the same bixbyite-type structure, the covalency of the Eu-O bond and the Eu site distortion increase with the difference of the ionic radii between europium and the cation of the host compound. The magnetic susceptibility, except for Sc_2O_3:Eu, follows the same evolution; it is explained by the increase of the term due to the crystal-field effect.

[1] M. Zachau and A. Konrad, Solid State Phenom. **99-100**, 13 (2004).
[2] J. L. Yuan and G. L. Wang, TRAC-Trend. Anal. Chem. **25**, 490 (2006).
[3] P. A. Tanner, J. Nanosci. Nanotechnol. **5**, 1455 (2005).
[4] K. Lebbou, P. Perriat, and O. Tillement, J. Nanosci. Nanotechnol. **5**, 1488 (2005).
[5] J. C. G. Bunzli and G. R. Choppin (Eds.), Lanthanoide Probes in Life, Chemical and Earth Sciences: Theory and Practice, Elsevier, Amsterdam 1989.
[6] F. Hanic, M. Hartmanova, G. G. Knab, A. A. Urusovskaya, and K. S. Bagdasarov, Acta Crystallogr. B **40**, 76 (1984).
[7] C. R. Stanek, K. J. McClennan, B. P. Uberuaga, K. E. Sickafus, M. R. Levy, and R. W. Grimes, Phys. Rev. B **75**, 134101 (2007).
[8] B. Antic, M. Mitric, and D. Rodic, J. Phys.: Condensed Matter **9**, 365 (1997).
[9] G. Concas, G. Spano, M. Bettinelli, and A. Speghini, Z. Naturforsch. **58a**, 551 (2003).
[10] G. Concas, G. Spano, E. Zych, and J. Trojan-Piegza, J. Phys.: Condensed Matter **17**, 2597 (2005).
[11] A. Grill and M. Schieber, Phys. Rev. B **1**, 2241 (1970).
[12] R. Krsmanovic, O. I. Lebedev, A. Speghini, M. Bettinelli, S. Polizzi, and G. Van Tendeloo, Nanotechnology **17**, 2805 (2006).
[13] F. Grandjean and G. J. Long, in: Mössbauer Spectroscopy Applied to Inorganic Chemistry, Vol. 3 (Eds. F. Grandjean and G. J. Long), Plenum Press, New York 1989, p. 513.
[14] G. Concas, F. Congiu, C. Muntoni, M. Bettinelli, and A. Speghini, Phys. Rev. B **53**, 6197 (1996).
[15] G. Concas, F. Congiu, G. Spano, A. Speghini, and K. Gatterer, J. Non-Cryst. Solids **232**, 341 (1998).
[16] P. Gütlich, R. Link, and A. Trautwein, Mössbauer Spectroscopy and Transition Metal Chemistry, Springer, Berlin 1978.
[17] H. T. Hintzen and H. M. van Noort, J. Phys. Chem. Solids **8**, 873 (1988).
[18] S. Polizzi, S. Bucella, A. Speghini, F. Vetrone, R. Naccache, J. C. Boyer, and J. A. Capobianco, Chem. Mater. **16**, 1330 (2004).
[19] S. Polizzi, G. Fagherazzi, M. Battagliarin, M. Bettinelli, and A. Speghini, J. Mater. Res. **16**, 146 (2001).
[20] P. Glentworth, A. L. Nichols, N. R. Large, and R. J. Bullock, J. Chem. Soc. Dalton Trans., 969 (1973).
[21] L. R. Morss, M. Siegal, L. Stenger, and N. Edelstein, Inorg. Chem. **9**, 1771 (1970).
[22] S. Margulies and J. R. Ehrman, Nucl. Instrum. Methods **12**, 131 (1961).
[23] G. K. Shenoy and B. D. Dunlap, Nucl. Instrum. Methods **71**, 285 (1969).
[24] J. C. Stevens, in: CRC Handbook of Spectroscopy, Vol. III (Ed. J. W. Robinson), CRC Press, Boca Raton 1981, p. 464.
[25] I. Nowik and I. Felner, Hyperfine Interact. **28**, 959 (1986).
[26] R. J. Hill and H. D. Flack, J. Appl. Crystallogr. **20**, 356 (1987).
[27] H. O'Connor and T. M. Valentine, Acta Crystallogr. **25**, 2140 (1969).
[28] R. D. Shannon, Acta Crystallogr. A **32**, 751 (1976).
[29] N. L. Huang and J. H. Van Vleck, J. Appl. Phys. **40**, 1144 (1969).
[30] R. R. Gupta, in: Landolt-Boernstein, Vol. II/16 (Eds. K. H. Hellwege and A. M. Hellwege), Springer, Berlin 1986, p. 402.
[31] S. Kern and R. Kostelecky, J. Appl. Phys. **42**, 1773 (1971).